REFERENCES

[1] J. D. Rhodes, "Direct design of symmetrical interacting bandpass channel diplexers," *Inst. Elec. Eng. J. Microwaves, Opt. Acous.*, vol. 1, no. 1, pp. 34–40, Sept. 1976.

[2] J. L. Haine and J. D. Rhodes, "Direct design formulas for asymmetric bandpass channel diplexers," *IEEE Trans. Microwave Theory Tech.*, vol. MTT-25, pp. 807–813, Oct. 1977.

[3] J. D. Rhodes and R. Levy, "General manifold multiplexers," this issue, pp. 111–123.

[4] J. D. Rhodes, *Theory of Electrical Filters*. New York: Wiley, 1976.

[5] R. J. Wenzel and W. G. Erlinger, "Narrowband contiguous multiplexing filters with arbitrary amplitude and delay response," *1976 IEEE MTT-S Int. Microwave Symp. Digest*, pp. 116–118.

[6] G. L. Matthaei and E. G. Cristal, "Theory and design of diplexers and multiplexers," in *Advances in Microwaves*, vol. 2, Leo Young, Ed. New York and London: Academic Press, 1967, pp. 237–326.

[7] R. Sato and E. G. Cristal, "Simplified analysis of coupled transmission-line networks," *IEEE Trans. Microwave Theory Tech., vol. MTT-18, pp.* 122–131, *Mar.* 1970.

[8] E. G. Cristal, "New design equations for a class of microwave filters," *IEEE Trans. Microwave Theory Tech.*, vol. MTT-19, pp. 486–490, May 1971.

Design of General Manifold Multiplexers

J. DAVID RHODES, MEMBER, IEEE, AND RALPH LEVY, FELLOW, IEEE

Abstract—**The direct analytical design process for arbitrary multiplexers given in a previous paper is extended to the case of bandpass channel filters connected to a uniform-impedance manifold (e.g., a length of waveguide or transmission line). The previous approximations are greatly improved by adding immittance compensation in a way which not only preserves the canonic form of the network but also assists in the physical construction by spacing the filters along a manifold. The phase shifters between channels are themselves sufficient to compensate the filter interactions to such an extent that contiguous channeling cases are designable. The results are presented mainly in closed form requiring minimal computer optimization.**

Analysis of multiplexers with frequency-dependent manifolds indicate that there are restrictions on the total bandwidth, but a ten-channel multiplexer is probably feasible, suitable for input and output multiplexers required in typical communications systems. Practical results on a simple manifold triplexer are presented.

I. INTRODUCTION

In the previous paper [1] it was shown that there are inherent limitations to the canonic matching of a multiplexer consisting of a number of filters connected directly in series or parallel. We may define canonic matching as that requiring only changes to the parameters of the filters and not adding extra immittance compensation networks. In this paper immittance compensation is introduced, but in a way which not only preserves the canonic form of the network but also assists in the physical construction by spacing the filters along a manifold. The phase shifters between channels are sufficient to compensate the multiplexer to such an extent that contiguous channeling cases are designable by the theory.

It is interesting to consider various approaches to the design of multiplexers, particularly on a manifold feed. Due to requirements in communication satellites and elsewhere, many attempts have been made to produce such multiplexers. One important and difficult requirement is that of an output multiplexer on a waveguide manifold with bandpass channels separated to yield guardbands of only 10 percent. Most design techniques have adopted an approach based upon singly terminated bandpass channels resulting in 3-dB crossover points between channels, e.g., [2], [3]. Such designs exhibit good return loss over the channel bandwidths and the guardbands. Also, dummy channels have to be included to simulate channels at the edges of the total multiplexer bandwidth, forming an additional annulling network. Thus redundant elements are necessary, and the channel interactions are compensated to produce a channel performance comparable to the individual channels based upon a singly terminated prototype.

The need for contiguous band multiplexers originally arose in receiver design for countermeasures where the incoming signal was unknown and complete band coverage was necessary with good match at all frequencies. Here all channels have to be designed on a singly terminated basis and must provide a prescribed level of attenuation over the major part of other bands.

However, the requirements for multiplexers in communication systems are different since they must provide

Manuscript received April 3, 1978; revised July 24, 1978.

J. D. Rhodes is with the Department of Electrical and Electronic Engineering, the University of Leeds, Leeds LS2 9JT, England.

R. Levy is with the Microwave Development Laboratories, Natick, MA 01760.

0018-9480/79/0200-0111$00.75 ©1979 IEEE

good reflection and transmission only over each channel bandwidth while maintaining high attenuation over all other channels. For typically realizable passband return loss specifications (e.g., 20–25 dB), the *optimum* solution leads to attenuation in excess of 10 dB at the crossover frequencies independent of the guardband bandwidth. Thus contiguous band multiplexers are *nonoptimum* in this situation and have probably been used because a design procedure was known. They result in a higher degree filter than necessary in each channel in addition to the annulling network. Furthermore, if one attempts to use singly terminated designs for crossover levels in excess of 3 dB, the passband return loss rapidly deteriorates if further annulling networks are not used.

The significant difference between the optimum design approach and the contiguously designed solution to the above type of problem may be illustrated by the simple diplexer examples presented in [4, Figs. 4 and 5]. For the case of two noncontiguous bandpass channels of bandwidth 2 and guardband of 1, five-cavity Chebyshev filters may produce a return loss >25 dB over each passband while >34-dB attenuation is achieved over the opposite channel [4, Fig. 4], whereas the contiguous approach using similar five-cavity filters gives an attenuation level over the opposite channel of only 19 dB [4, Fig. 5]. Thus the price paid for preserving the good 25-dB return loss at the common port over the guardband region is a 15-dB reduction in the attenuation level in the stopband! Hence, for most applications in communication systems, contiguous band multiplexers result in designs far from the optimum solution.

The alternative approach described here is an extension of the companion paper [1] and similarly commences from doubly terminated prototype filters. Modifications are then made to all elements when the manifold is designed. Criteria used in this approach are that multiplexers having an arbitrary number of channels with different bandwidths and variable center frequency spacings should be designable, and that the individual passband performances should be maintained from the case of large guardbands down to contiguous crossovers. In addition to the 6-dB improvement in stopband attenuation levels over frequency bands where a passband exists elsewhere in the multiplexer (given by any type of design due to power division between the in-band and out-of-band channels), further improvement in attenuation due to compensation of the interaction between channels should be expected.

II. Manifold Theory Applied to Frequency-Independent Manifolds

The theory for the manifold multiplexer is identical with that of the directly coupled multiplexer up to (15) and (17) of [1], which form the in-band and out-of-band input admittances of the channel filters. It is necessary to refer also to [1, Figs. 1–4] for definitions of the terminology. However, rather than employing direct parallel connection as in [1, Fig. 4], we form the manifold multiplexer

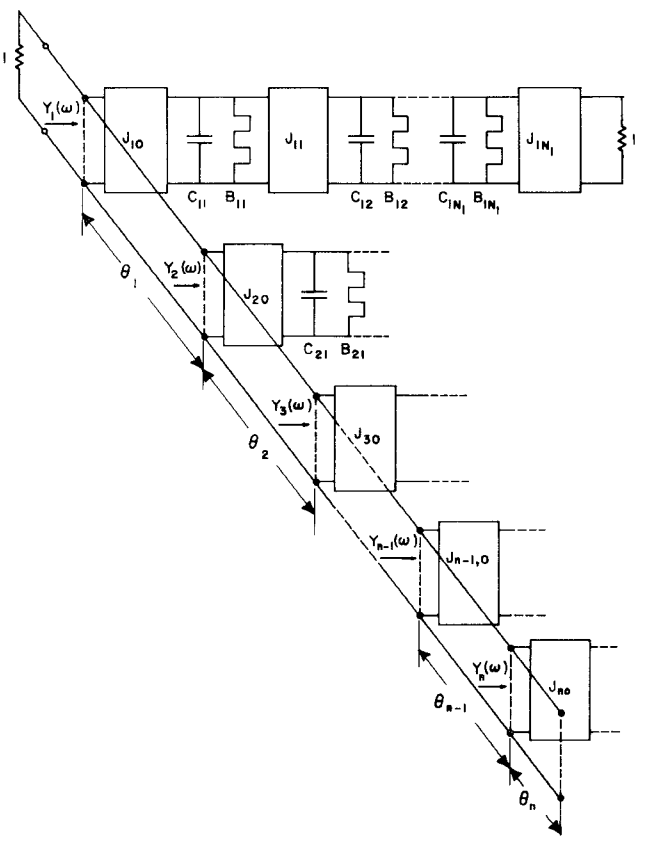

Fig. 1. Prototype manifold multiplexer.

shown in Fig. 1. $Y_m(\omega)$ is the imput admittance of the mth channel as a function of frequency. The transfer matrix of the mth, unity impedance phase shifter may be written as

$$\frac{1}{\sqrt{1+B_m^2\alpha^{-2}}}\begin{bmatrix} 1 & jB_m\alpha^{-1} \\ jB_m\alpha^{-1} & 1 \end{bmatrix} \tag{1}$$

where

$$\theta_m = \tan^{-1}\left(B_m\alpha^{-1}\right). \tag{2}$$

Initially the manifold is assumed to be frequency independent and of uniform inpedance. Modifications to the design process will be made at a later stage to account for the frequency dependence of the manifold. Note that as $\alpha\to\infty$ (the case of decoupled channels), $\theta_m\to 0$ or an integral multiple of π, i.e., the channels are effectively connected in parallel as in [1]. $\alpha=1$ gives the actual situation to be determined.

An additional n parameters $B_1, B_2, \cdots, B_n$ appear to have been obtained by connecting the filters on to a manifold, but later it will be shown that one of these is redundant.

If the rth channel is in band, then

$$Y_r = Y_r(\Omega_r\alpha + \omega_t) \tag{3}$$

as given by [1, eq. (15)] while the admittance of the rest of the channels which are out of band are given by

$$\overline{Y}_m = Y_m(\Omega_m\alpha + \omega_t) \tag{4}$$

with $m=1,\cdots,r-1,r+1,\cdots,n$ and $\bar{Y}_m$ is given by [1, eq. (17)]. The transfer matrix of the network at the set of frequencies $(\Omega_r\alpha+\omega_i)$ will now be derived. The transfer matrix for the mth channel admittance followed by the mth phase shifter is

$$[T_m]=\frac{1}{\sqrt{1+B_m^2\alpha^{-2}}}\cdot\begin{bmatrix}1 & jB_m\alpha^{-1}\\ jB_m\alpha^{-1}+\bar{Y}_m & 1+\dfrac{\alpha^{-2}B_m}{C_{m1}(\Omega_r-\Omega_m)}-\dfrac{\omega_i\alpha^{-3}B_m}{C_{m1}(\Omega_r-\Omega_m)^2}\end{bmatrix} \tag{5}$$

and the matrix possesses an error of order α^{-4}.

For the first $r-1$ channels we have a transfer matrix

$$\frac{1}{F}\begin{bmatrix}A & B\\ C & D\end{bmatrix}=\prod_{m=1}^{r-1}[T_m] \tag{6}$$

where by analysis, for errors up to α^{-4}, we have a lossless transfer matrix of the form

$$\begin{aligned}F&=1+\frac{1}{2}\sum_{m=1}^{r-1}B_m^2\alpha^{-2}\\ A&=1+a_1\alpha^{-2}-a_2\omega_i\alpha^{-3}\\ B&=j\sum_{m=1}^{r-1}B_m\alpha^{-1}+jb_1\alpha^{-3}\\ C&=j\sum_{m=1}^{r-1}B_m\alpha^{-1}+\sum_{m=1}^{r-1}\bar{Y}_m-jc_1\alpha^{-3}\\ D&=1+d_1\alpha^{-2}-\omega_i d_2\alpha^{-3}\end{aligned} \tag{7}$$

where

$$\begin{aligned}a_1&=\sum_{m=2}^{m-1}\frac{\sum_{i=1}^{m-1}B_i}{C_{m1}(\Omega_r-\Omega_m)}-\sum_{m=2}^{r-1}\left(B_m\sum_{i=1}^{m=1}B_i\right)\\ a_2&=\sum_{m=2}^{r-1}\frac{\sum_{i=1}^{m-1}B_i}{C_{m1}(\Omega_r-\Omega_m)^2}\\ b_1&=\sum_{m=2}^{r-1}B_m\cdot\left[\sum_{j=2}^{m}\frac{\sum_{i=1}^{j-1}B_i}{C_{j1}(\Omega_r-\Omega_j)}-\sum_{j=2}^{m-1}\left(B_j\sum_{i=1}^{j-1}B_i\right)\right]\\ c_1&=\sum_{m=2}^{r=1}\left[\left(\frac{1}{C_{m1}(\Omega_r-\Omega_m)}-B_m\right)\right.\\ &\quad\left.\cdot\left[\sum_{j=1}^{m=1}\frac{\sum_{i=j}^{m-1}B_i}{C_{j1}(\Omega_r-\Omega_j)}-\sum_{j=2}^{m=1}\left(B_j\cdot\sum_{i=1}^{j-1}B_i\right)\right]\right]\end{aligned}$$

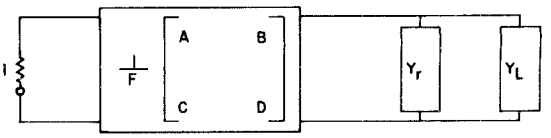

Fig. 2. Approximate equivalent circuit of manifold at frequencies in the rth-channel passband.

$$\begin{aligned}d_1&=\sum_{m=1}^{r-1}\frac{\sum_{i=m}^{r-1}B_i}{C_{m1}(\Omega_r-\Omega_m)}-\sum_{m=2}^{r-1}\left(B_m\cdot\sum_{i=1}^{m=1}B_i\right)\\ d_2&=\sum_{m=1}^{r=1}\frac{\sum_{i=m}^{r-1}B_i}{C_{m1}(\Omega_r-\Omega_m)^2}.\end{aligned} \tag{8}$$

We may proceed with a similar analysis for the network after the rth channel. However, we require only the input admittance which is given by

$$Y_L=\frac{C'}{A'} \tag{9}$$

with

$$\begin{aligned}A'&=1+a_1'\alpha^{-2}-a_2'\omega_i\alpha^{-3}\\ C'&=j\sum_{m=r}^{n}B_m\alpha^{-1}+\sum_{m=r+1}^{n}\bar{Y}_m-jC_1'\alpha^{-3}\end{aligned} \tag{10}$$

where

$$\begin{aligned}a_1'&=\sum_{m=r+1}^{n}\frac{\sum_{i=r}^{m-1}B_i}{C_{m1}(\Omega_r-\Omega_m)}-\sum_{m=r+1}^{n}\left(B_m\cdot\sum_{i=}^{m=1}B_i\right)\\ a_2'&=\sum_{m=r+1}^{n}\frac{\sum_{i=r}^{m-1}B_i}{C_{m1}(\Omega_r-\Omega_m)^2}\\ C_1'&=\sum_{m=r+2}^{n}\left[\left(\frac{1}{C_{m1}(\Omega_r-\Omega_m)}-B_m\right)\right.\\ &\quad\left.\cdot\left[\sum_{j=r+1}^{m}\frac{\sum_{i=4}^{m=1}B_i}{C_{j1}(\Omega_r-\Omega_j)}-\sum_{j=r+1}^{m}\left(B_j\cdot\sum_{i=r}^{j-1}B_i\right)\right]\right]\end{aligned} \tag{11}$$

and Y_L is a reactance function up to the order α^{-4}.

We now have the network shown in Fig. 2, and at the set of frequencies $\omega=\Omega_r\alpha+\omega_i$ we require the common port reflection coefficient and the rth channel port reflection coefficient to be zero. Since up to the order of approximation the networks given by (6) and (9) are lossless, we need only apply the condition of a conjugate match at any plane in the network. Applying this condition at the junction with the rth port we have

$$Y_r=\frac{A-C}{D-B}-\frac{C'}{A'}. \tag{12}$$

Expanding the right-hand side of the equation as a power series in α^{-1} and comparing with the expansion of Y_r in [1, (15)] yields

1) α^{-1} *term:*

$$C_{r1}\beta_{r11} = \sum_{m=1\neq r}^{n} \frac{1}{C_{m1}(\Omega_r - \omega m)} - \sum_{m=r}^{n} B_m \tag{13}$$

2) $\alpha^{-2}\omega_t$ *term:*

$$\gamma_{r12}C_{r1} = \sum_{m=1\neq r}^{n} \frac{1}{C_{m1}(\Omega_r - \Omega_m)^2} \tag{14}$$

3) α^{-2} *term:*

$$\gamma_{r12} - \gamma_{r02} - C_r^2 1\beta_{r11}^2 = a_1 - d_1 - \sum_{m=1}^{r-1} B_m \cdot \sum_{m=1}^{r-1} \frac{1}{C_{m1}(\Omega_r - \Omega_m)} \tag{15}$$

4) $\alpha^{-3}\omega_t^2$ *term:*

$$\frac{C_{r1}^2 C_{r2}\beta_{r23}}{J_{r1}^2} = \sum_{m=1\neq r}^{n} \frac{1}{C_{m1}(\Omega_r - \Omega_m)^3} \tag{16}$$

5) $\alpha^{-3}\omega_t$ *term:*

$$\frac{-2C_{r1}C_{r2}\beta_{r23}}{J_{r1}^2} + 2C_{r1}^2\beta_{r11}\gamma_{r12} = d_2 - a_2 + \sum_{m=1}^{r-1} B_m \cdot \sum_{m=1}^{r-1} \frac{1}{C_{m1}(\Omega_r - \Omega_m)^2} \tag{17}$$

6) α^{-3} *term:*

$$C_{r1}\beta_{r13} - \frac{C_{r2}\beta_{r23}}{J_{r1}^2} + 2C_{r1}\beta_{r11}\gamma_{r12} - \gamma_{r02}C_{r1}\beta_{r11} - C_{r1}^3\beta_{r11}^3 = \sum_{m=1\neq r}^{n} \left[\frac{1}{C_{m1}(\Omega_r - \Omega_m)} \left(-\gamma_{m02} + \frac{\beta_{m11}}{(\Omega_r - \Omega_m)} + \frac{J_{m1}^2}{C_{m1}C_{m2}(\Omega_r - \Omega_m)^2} \right) \right] + c_1 + c_1' - a_1' \cdot \sum_{m=r+1}^{n} \frac{1}{C_{m1}(\Omega_r - \Omega_m)} + a_1' \sum_{m=r}^{n} B_m + b_1 - d_1 \sum_{m=1}^{r-1} \frac{1}{C_{m1}(\Omega_r - \Omega_m)} + (a_1 + d_1) \sum_{m=1}^{r-1} B_m - \left(\sum_{m=1}^{r-1} B_m \right)^2 \sum_{m=1}^{r-1} \frac{1}{C_{m1}(\Omega_r - \Omega_m)} \cdot \tag{18}$$

Applying the above set of equations for $r = 1 \rightarrow n$ leads to $6n$ equations with up to $6n$ unknowns. Since these are linear simultaneous equations we may attempt to obtain direct expressions for the unknown quantities.

Substituting for a_2 and d_2 from (8) into (17) gives

$$\frac{-C_{r1}C_{r2}\beta_{r23}}{J_{r1}^2} + C_{r1}^2\beta_{r11}\gamma_{r12} = \sum_{m=1}^{r-1} \frac{\sum_{\iota=m}^{r-1} B_\iota}{C_{m1}(\Omega_r - \Omega_m)^2} \cdot \tag{19}$$

Defining a new function P_r as

$$P_r = \sum_{m=1\neq r}^{n} \frac{1}{C_{m1}(\Omega_r - \Omega_m)^2} \cdot \sum_{m=1\neq r}^{n} \frac{1}{C_{m1}(\Omega_r - \Omega_m)} - \frac{1}{C_{r1}} \cdot \sum_{m=1\neq r}^{n} \frac{1}{C_{m1}(\Omega_r - \Omega_m)^3} \tag{20}$$

and substituting for β_{r23} and γ_{r12} from (16) and (14), respectively, into (19) results in the set of equations

$$P_r - \sum_{m=r}^{n} B_m \cdot \sum_{m=1\neq r}^{n} \frac{1}{C_{m1}(\Omega_r - \Omega_m)^2} = \sum_{m=1}^{r-1} \frac{\sum_{\iota=m}^{r-1} B_\iota}{C_{m1}(\Omega_r - \Omega_m)^2} \qquad (r = 1, 2, \cdots, n). \tag{21}$$

If

$$H_r = \sum_{m=r}^{n} B_m \tag{22}$$

then (21) may be rearranged as

$$H_r = \frac{P_r - \sum_{m=1}^{r-1} \frac{H_m}{C_{m1}(\Omega_r - \Omega_m)^2}}{\sum_{m=r+1}^{n} \frac{1}{C_{m1}(\Omega_r - \Omega_m)^2}} \tag{23}$$

and hence H_r may be obtained for $r = 1 \rightarrow n-1$. H_n is, in general, indeterminate since the set of equations (21) on close inspection represent n equations with $n-1$ unknowns. From a network viewpoint this may readily be appreciated by considering the network shown in Fig. 1. The last phase shifter θ_n represents a frequency invariant reactance in parallel with the nth channel admittance $Y_n(\omega)$. Since this may be readily absorbed into the modification to the first admittance inverter and resonant frequency of the first cavity, this element is redundant and may be made zero, i.e.,

$$B_n = 0. \tag{24}$$

In the very special case of the diplexer

$$P_1 = \frac{(C_{11} - C_{12})}{C_{11}C_{12}^2(\Omega_1 - \Omega_2)^2} \qquad P_2 = \frac{C_{12}}{C_{11}} P_1 \tag{25}$$

and, consequently,

$$P_2 - \frac{H_1}{C_{11}(\Omega_2 - \Omega_1)^2} = 0 \tag{26}$$

enabling both equations given in (21) to be satisfied. For

the triplexer and above in the nth channel at the end of the manifold only five of the six conditions may be satisfied.

Combining (22) and (24) we have the final design for the manifold

$$B_r = H_r - H_{r+1} \tag{27}$$

with $r=1,2,\cdots,n-1$ and $H_n=0$.

Having solved for B_r, we may then substitute into (13) to obtain β_{r11} as

$$\beta_{r11} = \frac{1}{C_{r1}}\left[\sum_{m=1\neq r}^{n} \frac{1}{C_{m1}(\Omega_r-\Omega_m)} - \sum_{m=r}^{n} B_m\right] \tag{28}$$

and from (14) and (16)

$$\gamma_{r12} = \frac{1}{C_{r1}} \sum_{m=1\neq r}^{n} \frac{1}{C_{m1}(\Omega_r-\Omega_m)^2} \tag{29}$$

and

$$\beta_{r23} = \frac{J_{r1}^2}{C_{r1}^2 C_{r2}} \sum_{m=1\neq r}^{n} \frac{1}{C_{m1}(\Omega_r-\Omega_m)^3}. \tag{30}$$

Additionally, the substitution of (8) into (15) gives

$$\gamma_{r02} = \gamma_{r12} - C_{r1}^2\beta_{r11}^2 + 2\sum_{m=1}^{r-1} \frac{\sum_{i=m}^{r-1} B_i}{C_{m1}(\Omega_r-\Omega_m)}. \tag{31}$$

In principle, the set of equations (18) may be used to obtain β_{r13}, but these contain very tedious algebra. Since these equations result from the α^{-3} term, they represent a fine adjustment to the matching of each channel around midband, and, in general, this is more readily done by direct computer optimization of the circuit around the midband frequencies of each channel, as described later. Furthermore, since the $\alpha^{-3}\omega_i$ could not be satisfied for the nth channel, such optimization leads to a slightly improved performance.

A further fine improvement in the design formulas may be obtained by closer inspection of the expansions for Y_r and Y_m as given in [1, eqs. (15) and (17)]. If we assume that the resonant frequencies of all the resonators should be changed, then noting the format of [1, (11)], the following generalization is applied:

$$B_{rk} \rightarrow -C_{rk}(\Omega_r\alpha + \beta_{rkl}\alpha^{-l}) \tag{32}$$

where $l=2k-1$, $k=2,3,\cdots,N_r$. Similarly, if we assume that the admittance inverters should also change, then a generalization of [1, (9)] leads to

$$J_{rk}^2 \rightarrow J_{rk}^2(1-\gamma_{rkl}\alpha^{-l}) \tag{33}$$

where $l=2k$, $k=1,2,\cdots,N_r-1$. Now by expanding [1, (15) and (17)] to α^{-5} it becomes obvious that the extra correction terms above are associated only with the terms of highest degree in ω_i for each coefficient of α^{-l}. Thus in addition to [1, (19), (20), and (22)] which give

1) $\alpha^{-1}\omega_i^0$ *term:*

$$\beta_{r11} = \frac{1}{C_{r1}} \sum_{m=1\neq r}^{n} \frac{1}{C_{m1}(\Omega_r-\Omega_m)} \tag{34}$$

2) $\alpha^{-2}\omega_i$ *term:*

$$\gamma_{r12} = \frac{1}{C_{r1}} \sum_{m=1\neq r}^{n} \frac{1}{C_{m1}(\Omega_r-\Omega_m)^2} \tag{35}$$

3) $\alpha^{-3}\omega_i^2$ *term:*

$$\beta_{r23} = \frac{J_{r1}^2}{C_{r1}^2 C_{r2}} \sum_{m=1\neq r}^{n} \frac{1}{C_{m1}(\Omega_r-\Omega_m)^3} \tag{36}$$

we have also

4) $\alpha^{-4}\omega_i^3$ *term:*

$$\gamma_{r24} = \frac{J_{r1}^2}{C_{r1}^2 C_{r2}} \sum_{m=1\neq r}^{n} \frac{1}{C_{m1}(\Omega_r-\Omega_m)^4} \tag{37}$$

and

5) $\alpha^{-5}\omega_i^4$ *term:*

$$\beta_{r35} = \frac{J_{r1}^2 J_{r2}^2}{C_{r1}^2 C_{r2}^2 C_{r3}} \sum_{m=1\neq r}^{n} \frac{1}{C_{m1}(\Omega_r-\Omega_m)^5}. \tag{38}$$

The general expression for the higher order terms is now obvious. Actually, these are associated with the effect of the first resonators only of each out-of-band channel, since such resonators are responsible for the terms of highest degree in ω_i.

At this point it is useful to summarize the design process step-by-step.

1) Compute the values of P_r given by (20).

2) Compute the values of H_r given by (23) for $r=1,2,\cdots,n-1$ and $H_n=0$.

3) Then the B_r are given by (27).

4) The coefficients β_{r11}, γ_{r12}, β_{r23}, and γ_{r02} are given by (28)–(31).

5) The higher ordered correction terms γ_{rkl} with $l=2k$ and β_{rkl} with $l=2k-1$ which are defined in (32) and (33) are given by formulas such as (37) and (38), which are easily generalized to give

$$\gamma_{rkl} = \frac{1}{C_{rk}}\left(\prod_{s=1}^{k-1} \frac{J_{rs}^2}{C_{rs}^2}\right) \sum_{m=1\neq r}^{n} \frac{1}{C_{m1}(\Omega_r-\Omega_m)^l} \tag{39}$$

where $l=2k$ and

$$\beta_{rkl} = \frac{1}{C_{rk}}\left(\prod_{s=1}^{k-1} \frac{J_{rs}^2}{C_{rs}^2}\right) \sum_{m=1\neq r}^{n} \frac{1}{C_{m1}(\Omega_r-\Omega_m)^l} \tag{40}$$

where $l=2k-1$.

As stated earlier, in addition to the above design process, a further refinement may be made to ensure that the best possible performance is obtained about the band center frequencies. For out-of-band channels, one may truncate the filters after two or three cavities to produce a

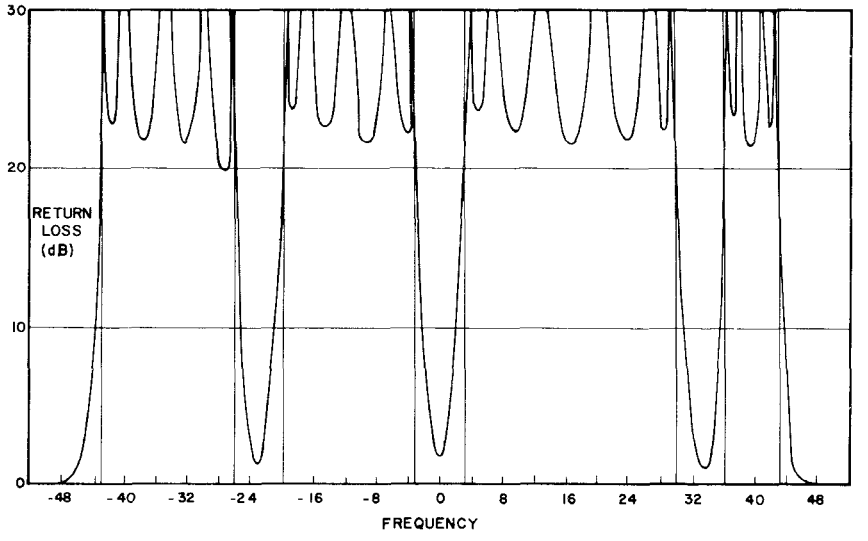

Fig. 3. Computer response for common port return loss of the four-channel manifold multiplexer.

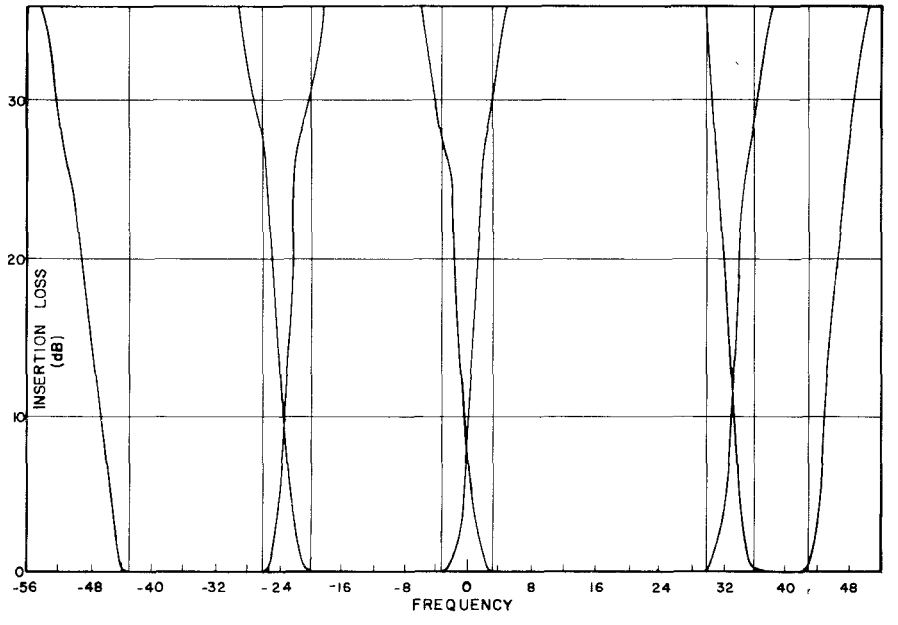

Fig. 4. Insertion loss response for each channel of the four-channel manifold multiplexer.

purely reactive loading on the manifold. Define Ω_{rk} as the resonant frequency of the kth resonator of channel r. Then in the odd-degree case J_{r0} and Ω_{r1} may be slightly modified to produce a conjugate match at the junction with the manifold at midband. For the even-degree case, J_{r1} and Ω_{r2} in addition may be modified to produce a conjugate match at the two frequencies closest to midband. This updating process may be performed channel by channel and, if necessary, may be repeated.

A computer program has been developed to evaluate all of the design formulas with the additional updating process described above. As an example, we may consider a four-channel prototype multiplexer with all channels being of the conventional Chebyshev type. The first channel to be dropped along the manifold from the common port is of fifth degree,[1] passband return loss of 22 dB, bandwidth 17, and center frequency -34.5. The three remaining channels in order are of degree 5, 6, and 4, bandwidths 17, 27, and 7, and center frequencies -11.5, 16.5, and 39.5, all designed with a passband return loss of 22 dB. The guardband between all channels is 6. This multiplexer has much closer relative channel spacings than any of the designs illustrated in [1]. The element values are given in Table I, and the computed response for the common port return loss is shown in Fig. 3 with the return loss at the appropriate channel port being comparable over the corresponding passband. The performance is

[1]Here "degree" corresponds to the number of cavities or resonant elements of the filter.

TABLE I
TABLE OF ELEMENT VALUES OF FOUR-CHANNEL PROTOTYPE MULTIPLEXERS "COUPLING" IS J_{rk}, "ADM" IS C_{rk}, AND "RES. FREQ." IS Ω_{rk}; ELEMENTS ADJACENT TO THE MANIFOLD ARE TABULATED FIRST

CHANNEL	DEGREE	RET.LOSS	BANDWIDTH	CENTRE FREQ.
1	5	22 dB	17	-34.5
COUPLING	ADM.	RES.FREQ.		
0.9665	0.1053	-37.9807		
1.1825	0.2757	-35.0087		
1.6849	0.3408	-34.5264		
1.7011	0.2757	-34.5015		
1.3132	0.1053	-34.5002		
CHANNEL	DEGREE	RET.LOSS	BANDWIDTH	CENTRE FREQ.
2	5	22 dB	17	-11.5
COUPLING	ADM.	RES.FREQ.		
1.0119	0.1053	-13.2129		
1.1246	0.2757	-11.4549		
1.6747	0.3408	-11.4894		
1.7007	0.2757	-11.4991		
1.3112	0.1053	-11.4999		
CHANNEL	DEGREE	RET.LOSS	BANDWIDTH	CENTRE FREQ.
3	6	22 dB	27	16.5
COUPLING	ADM.	RES.FREQ.		
1.6159	0.0680	4.1212		
1.2041	0.1859	16.9914		
1.7760	0.2539	16.4915		
2.0294	0.2539	16.4953		
1.8376	0.1859	16.4991		
1.3367	0.0680	16.4997		
CHANNEL	DEGREE	RET.LOSS	BANDWIDTH	CENTRE FREQ.
4	4	22 dB	7	39.5
COUPLING	ADM.	RES.FREQ.		
0.7698	0.2440	42.5573		
1.2298	0.5890	39.6479		
1.4964	0.5890	39.5007		
1.2737	0.2440	39.5		
MANIFOLD PHASE SHIFTERS (RADIANS)				
-0.3181	-0.8026	0.7818		

very close to the 22-dB return loss level, and the bandwidths and center frequencies are equal to the original channel requirements. The significant improvement in channel performance using this multiplexer design may be observed in Fig. 4 where the insertion loss of each channel is plotted. The 28-dB minimum level of attenuation of the first three channels and 38 dB for the fourth channel over all other channels are 10 dB larger than would have been achieved by the channels operating in isolation. Alternatively, this may be viewed as a saving of one cavity per channel over using individual channel filters and other channel combination procedures to meet the same specification. Many examples have been analyzed, and it has been found that there is very little deterioration in return loss performance even down to contiguous channels.

In most practical realizations of this prototype multiplexer, the manifold will have phase properties which are frequency dependent. We shall consider in detail the case where the manifold possesses a transmission-line frequency dependence, and any other cases could be considered in a similar manner.

III. THE FREQUENCY DEPENDENT MANIFOLD

Incorporation of the frequency dependence of the manifold in a manner compatible with the established design procedure is by no means obvious. The problem is to incorporate correction terms α^{-r} into the circuit description of a length of transmission line in a way which is both physically reasonable and results in a tractable solution. A number of early attempts failed for reasons which became apparant only after successful solutions were obtained.

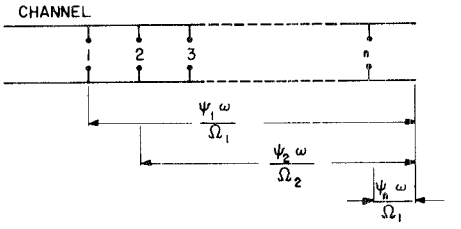

Fig. 5. Definition of phase lengths in manifold.

The first positive results were obtained using a piecewise-constant expression for the phase shift between channels. This is equivalent to an assumption that the individual channel bandwidths are sufficiently small so over any one channel the manifold presents a constant phase shift to the network. Over different channels the manifold possesses different constant values of phase shift.

This approach gives a considerable improvement over the constant phase shifter prototype when implemented into the design equations and applied to practical situations. However, with several channels requiring a long manifold the response deteriorates due to large phase changes of the manifold across the individual channel passbands. It is necessary then to take the frequency dependence of the manifold into account more exactly as follows.

The manifold multiplexer shown schematically in Fig. 5 indicates shunt-connected channels terminated in an open-circuited line. The electrical length between the rth channel and the termination is defined as ψ_r at the frequency Ω_r, leading to the general expressions indicated in the figure valid at any frequency ω. This circuit may be regarded as a prototype, and practical cases using a short-circuit termination may be designed by including slight modifications as described later.

In the constant phase-shifter theory, the transfer matrix of a phase shifter between physically adjacent channels was defined as in (1) and (2). In the frequency-dependent case, it is recognized that the most dominant terms involved in the design equations will be the lengths from each channel to the termination rather than the interchannel spacings. The following transfer matrix is found to give an adequate representation of the mth electrical length (shown in Fig. 5):

$$T(\psi_m) = \frac{1}{\sqrt{1+\alpha^{-2}\tan^2\left(\frac{\psi_m \alpha^{-1}\omega}{\Omega_m}\right)}} \cdot \begin{bmatrix} 1 & j\alpha^{-1}\tan\left(\frac{\psi_m \alpha^{-1}\omega}{\Omega_m}\right) \\ j\alpha^{-1}\tan\left(\frac{\psi_m \alpha^{-1}\omega}{\Omega_m}\right) & 1 \end{bmatrix}. \quad (41)$$

When $\alpha=1$, this matrix represents a length of transmission line. It has the same format as (1) and (2) with the susceptance B_m replaced by $\tan(\psi_m\omega\cdot\alpha^{-1}/\Omega_m)$. Hence the transformation $\alpha\rightarrow-\alpha$ does not change the sign of the electrical length (the B and C terms in (41) do not change sign), which is a physical requirement. It is known that the distance of each channel to the termination is close to an integral multiple of π even for channels spaced fairly closely in frequency, so that the transfer matrix (41) should not vary too rapidly with changes in interchannel frequencies (i.e., with changes in α). The essentially quadratic (α^{-2}) dependence of this transfer matrix ensures that the transfer matrix does indeed vary slowly with α and results in physically valid solutions.

The transfer matrix between channels m and $m+1$ is, by application of (41), given by

$$T(\psi_m)T(-\psi_{m+1})$$

$$=\frac{1}{\sqrt{1+\alpha^{-2}\tan^2\phi_m}}\begin{bmatrix}1 & j\alpha^{-1}\tan\phi_m\\ j\alpha^{-1}\tan\phi_m & 1\end{bmatrix}$$

$$\cdot\frac{1}{\sqrt{1+\alpha^{-2}\tan^2\phi_{m+1}}}\begin{bmatrix}1 & j\alpha^{-1}\tan\phi_{m+1}\\ j\alpha^{-1}\tan\phi_{m+1} & 1\end{bmatrix}$$

$$=\frac{1}{\sqrt{1+\alpha^{-2}B_m^2}}\begin{bmatrix}1 & j\alpha^{-1}B_m\\ j\alpha^{-1}B_m & 1\end{bmatrix} \quad (42)$$

where at $\omega=\Omega_r\alpha+\omega_i$

$$\phi_m=\frac{\psi_m}{\Omega_m}(\Omega_r+\omega_i\alpha^{-1})$$

$$\phi_{m+1}=\frac{\psi_{m+1}}{\Omega_{m+1}}(\Omega_r+\omega_i\alpha^{-1}) \quad (43)$$

$$B_m=\frac{\tan\phi_m-\tan\phi_{m+1}}{1+\alpha^{-2}\tan\phi_m\tan\phi_{m+1}}. \quad (44)$$

This implies that in the previous analysis for the frequency independent manifold as presented in Section II, B_m should be replaced by the expression (44) above, after expansion as a power series in α^{-1}. Thus in the previous analysis we should replace the following quantities containing B_m by the expressions shown:

$$\alpha^{-1}\sum_{m=1}^{r-1}B_m=\alpha^{-1}\left(\tan\left(\frac{\psi_1}{\Omega_1}\Omega r\right)-\tan(\psi_r)\right)$$

$$+\omega_i\alpha^{-2}\left(\frac{\psi_1}{\Omega_1}\left(1+\tan^2\left(\frac{\psi_1}{\Omega_1}\Omega_r\right)\right)-\frac{\psi_r}{\Omega_r}(1+\tan^2\psi_r)\right)$$

$$+\alpha^{-3}\left(G_r+\omega_i^2\left[\left(\frac{\psi_1}{\Omega_1}\right)^2\tan\left(\frac{\psi_1}{\Omega_1}\Omega_r\right)\left(1+\tan^2\left(\frac{\psi_1}{\Omega_1}\Omega_r\right)\right)\right.\right.$$

$$\left.\left.-\left(\frac{\omega_r}{\Omega_r}\right)^2\tan\psi_r(1+\tan^2\psi_r)\right]\right)+\epsilon(\alpha^{-4}) \quad (45)$$

and

$$\alpha^{-1}\sum_{m=r}^{n}B_m=\alpha^{-1}\tan\psi_r+\omega_i\alpha^{-2}\frac{\psi_r}{\Omega_r}(1+\tan^2\psi_r)$$

$$+\alpha^{-3}\left(G_r'+\omega_i^2\left(\frac{\psi_r}{\Omega_r}\right)^2\tan\psi_r(1+\tan^2\psi_r)\right)+\epsilon(\alpha^{-4}). \quad (46)$$

Here G_r, G_r' are undetermined coefficients of α^{-3} which are not required.

If the analysis of the manifold is modified accordingly, then (13)–(17) become

α^{-1} term:

$$C_{r1}\beta_{r11}=\sum_{m=1}^{n}{}_{\neq r}\frac{1}{C_{m1}(\Omega_r-\Omega_m)}-\tan\psi_r \quad (47)$$

$\alpha^{-2}\omega_i$ term:

$$\gamma_{r12}C_{r1}=\sum_{m=1}^{n}{}_{\neq r}\frac{1}{C_{m1}(\Omega_r-\Omega_m)^2}+\frac{\psi_r}{\Omega_r}(1+\tan^2\psi_r) \quad (48)$$

α^{-2} term:

$$\gamma_{r02}=\gamma_{r12}-C_{r1}^2\beta_{r11}^2+2\sum_{m=1}^{r-1}\frac{\tan\left(\frac{\psi_m}{\Omega_m}\Omega_r\right)-\tan(\psi_r)}{C_{m1}(\Omega_r-\Omega_m)}$$

(see also (31)) (49)

$\alpha^{-3}\omega_i^2$ term:

$$\frac{C_{r1}^2C_{r2}\beta_{r23}}{J_{r1}^2}=\sum_{m=1\neq r}^{n}\frac{1}{C_{m1}(\Omega_r-\Omega_m)^3}-\left(\frac{\psi_r}{\Omega_r}\right)^2$$

$$\cdot\tan\psi_r(1+\tan^2\psi_r) \quad (50)$$

$\alpha^{-3}\omega_i$ term:

$$\frac{-2C_{r1}C_{r2}\beta_{r23}}{J_{r1}^2}+2C_{r1}^2\beta_{r11}\gamma_{r12}$$

$$=d_2-\alpha_2+\left(\tan\left(\frac{\psi_1}{\Omega_1}\cdot\psi_r\right)-\tan\psi_r\right)\cdot\sum_{m=1}^{r-1}\frac{1}{C_{m1}(\Omega_r-\Omega_m)^2}$$

$$-\left(\frac{\psi_1}{\Omega_1}\left(1+\tan^2\left(\frac{\psi_1}{\Omega_1}\cdot\Omega_r\right)\right)\right.$$

$$\left.-\frac{\psi_r}{\Omega_r}(1+\tan^2\psi_r)\right)\sum_{m=1}^{r-1}\frac{1}{C_{m1}(\Omega_r-\Omega_m)}$$

$$+\sum_{m=2}^{r-1}\frac{\frac{\psi_1}{\Omega_1}\left(1+\tan^2\left(\frac{\psi_1}{\Omega_1}\Omega_r\right)\right)-\frac{\psi_m}{\Omega_m}\left(1+\tan^2\left(\frac{\psi_m}{\Omega_m}\Omega r\right)\right)}{C_{m1}(\Omega_r-\Omega_m)}$$

$$-\sum_{m=1}^{r-1}\frac{\frac{\psi_m}{\Omega_m}\left(1+\tan^2\left(\frac{\psi_m}{\Omega_m}\Omega_r\right)\right)-\frac{\psi_r}{\Omega_r}(1+\tan^2\psi_r)}{C_{m1}(\Omega_r-\Omega_m)} \quad (51)$$

which reduces to

$$-\frac{C_{r1}C_{r2}\beta_{r23}}{J_{r1}^2}+C_{r1}^2\beta_{r11}\gamma_{r12}=\sum_{m=1}^{r-1}\frac{\tan\left(\frac{\psi_m}{\Omega_m}\Omega_r\right)-\tan\psi_r}{C_{m1}(\Omega_r-\Omega_m)^2}$$
$$-\sum_{m=1}^{r-1}\frac{\frac{\psi_m}{\Omega_m}\left(1+\tan^2\left(\frac{\psi_m}{\Omega_m}\cdot\Omega_r\right)\right)-\frac{\psi_r}{\Omega_r}(1+\tan^2\psi_r)}{C_{m1}(\Omega_r-\Omega_m)}. \quad (52)$$

Substituting (47), (48), and (50) into (52) gives

$$P_r=\tan\psi_r\cdot\sum_{m=r+1}^{n}\frac{1}{C_{m1}(\Omega_r-\Omega_m)^2}$$
$$-\frac{\psi_r}{\Omega_r}(1+\tan^2\psi_r)\cdot\sum_{m=r+1}^{n}\frac{1}{C_{m1}(\Omega_r-\Omega_m)}$$
$$+\frac{\psi_r}{\Omega_r}\tan\psi_r(1+\tan^2\psi_r)$$
$$-\frac{1}{C_{r1}}\left(\frac{\psi_r}{\Omega_r}\right)^2\tan\psi_r(1+\tan^2\psi_r)$$
$$+\sum_{m=1}^{r-1}\frac{\tan\left(\frac{\psi_m}{\Omega_m}\Omega_r\right)}{C_{m1}(\Omega_r-\Omega_m)^2}-\sum_{m=1}^{r-1}\frac{\frac{\psi_m}{\Omega_m}\left(1+\tan^2\left(\frac{\psi_m}{\Omega_m}\Omega r\right)\right)}{C_{m1}(\Omega_r-\Omega_m)} \quad (53)$$

where P_r is defined in (20).

For large phase lengths in the manifold, the second and sixth terms on the right-hand side of this equation can become large. These terms, however, were obtained from a power series expansion in α^{-1} which assumed that these were small as compared to the first and fifth terms. Thus it is important to recombine the terms.

Consider the function

$$\tan\left(\frac{\Omega_m}{\Omega_r}\psi_r\right)=\tan\left(\psi_r+(\Omega_m-\Omega_r)\frac{\psi_r}{\Omega_r}\right). \quad (54)$$

Assuming that $(1-\Omega_m/\Omega_r)$ is small as compared to unity, we may expand (54) as a power series in $(\Omega_m-\Omega_r)$. The first three terms are

$$\tan\left(\frac{\Omega_m}{\Omega_r}\psi_r\right)=\tan\psi_r+(\Omega_m-\Omega_r)$$
$$\cdot\frac{\psi_r}{\Omega_r}(1+\tan^2\psi_r)+(\Omega_m-\Omega_r)^2$$
$$\cdot\left(\frac{\psi_r}{\Omega_r}\right)^2\tan\psi_r(1+\tan^2\psi_r)+\cdots. \quad (55)$$

Hence the first four terms of the right-hand side of (53) may be combined into the form

$$\sum_{m=r+1}^{n}\frac{\tan\left(\frac{\Omega_m}{\Omega_r}\psi_r\right)}{C_{m1}(\Omega_r-\Omega_m)^2}+\left(1-\frac{\psi_r}{\Omega_r}\sum_{m=r}^{n}\frac{1}{C_{r1}}\right)$$
$$\cdot\frac{\psi_r}{\Omega_r}\tan\psi_r(1+\tan^2\psi_r). \quad (56)$$

Combining terms five and six on the right-hand side of (53) in a similar manner results in (53) becoming

$$P_r=\sum_{m=r+1}^{n}\frac{\tan\left(\frac{\Omega_m}{\Omega_r}\psi_r\right)}{C_{m1}(\Omega_r-\Omega_m)^2}+\left(1-\frac{\psi_r}{\Omega_r}\sum_{m=r}^{n}\frac{1}{C_{r1}}\right)$$
$$\cdot\frac{\psi_r}{\Omega_r}\tan\psi_r(1+\tan^2\psi_r)+\sum_{m=1}^{r-1}\frac{\tan\psi_m}{C_{m1}(\Omega_r-\Omega_m)^2}$$
$$-\sum_{m=1}^{r-1}\left(\frac{\psi_m}{\Omega_m}\right)^2\frac{1}{C_{m1}}\tan\psi_m(1+\tan^2\psi_m). \quad (57)$$

In practice, the terms in (57) containing the $(\psi_m/\Omega_m)^2$ factors may now be deleted.

For $r=1$, the only unknown appearing in this transcendental equation is ψ_1 which may be obtained iteratively using, for example, the Newton–Raphson technique for a solution around any integral number of π rad.

Having obtained ψ_1, (57) may then be solved for ψ_2 with $r=2$ under the restriction

$$\frac{\psi_r}{\Omega_r}<\frac{\psi_{r-1}}{\Omega_{r-1}} \quad (58)$$

which is necessary to ensure that a positive length of line separates the two channels along the manifold. This process may be repeated until $r=n-1$, but for $r=n$ the first term on the right-hand side of (57) disappears, and a solution to the equation may be difficult to obtain. This corresponds closely to the result obtained in the frequency independent manifold case. Normally ψ_n would be chosen to be zero.

From the values of ψ_r, (47)–(50) may then be used to obtain the remaining design parameters, and a simple updating process commencing with the nth channel will ensure a good passband match near to the band center of each channel.

Frequently it may be desirable to terminate the manifold in a short circuit approximately $\pi/2$ rad from the last channel. This is achieved readily by replacing

$$\tan\theta\rightarrow-\cot\theta=\tan\left(\theta-\frac{\pi}{2}\right) \quad (59)$$

in (47)–(57) resulting in an increase in each value of ψ_r by approximately $\pi/2$.

These equations have been programmed and applied to the design of several multiplexers having either widely spaced or contiguous channels. As an example of the latter a ten-channel manifold was designed in WR75 to

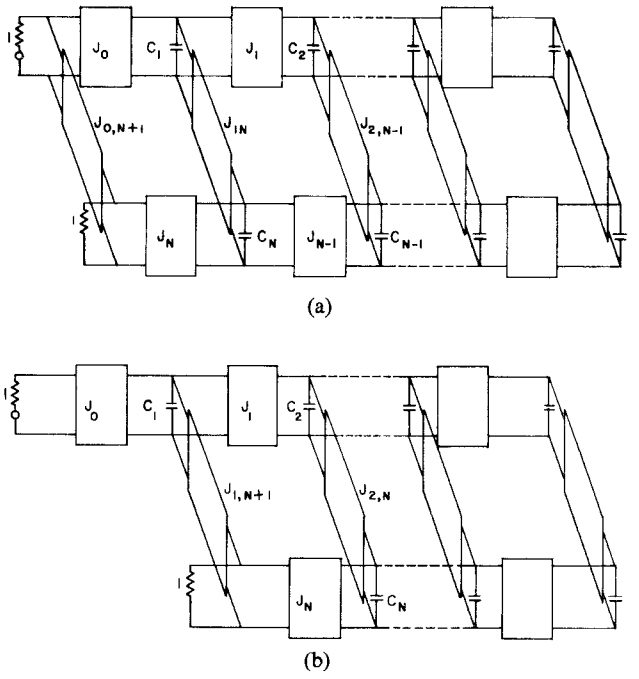

Fig. 6. (a) Realization of general even-degree filter. (b) Realization of general odd-degree filter.

divide the 14–14.5-GHz band into ten contiguous channels. The doubly terminated prototype filters were selected to have six cavities with 22-dB return loss bandwidth of 43 MHz, and the channel center frequencies were spaced by 49 MHz (this gives 3-dB crossover points). The multiplexer synthesized from the design equations was analyzed on the computer, and showed results in good agreement with theory. In fact, the worst return loss at the common port in the entire band is approximately 16 dB, occurring near the passband edges; most of the band has return loss of greater than 22 dB. This multiplexer has not yet been built in practice, but there is good reason to believe that practical versions would work in accordance with theory, since the computer analysis is known to be accurate in predicting practical performance. Presently only relatively simple manifold multiplexers, such as that described in Section IV, have been actually constructed.

A. Extension to Filters with Extra Cross-Couplings

In the most general case of optimum equiripple filters having finite frequency transmission zeros and/or complex conjugate pairs of transmission zeros giving improved phase response, extra cross-couplings are utilized as designated by the cross-coupling admittance inverters included in the low-pass prototypes depicted in Fig. 6. The even-degree case is shown in Fig. 6(a), and the convenient asymmetric realization of the odd-degree case [5] is shown in Fig. 6(b). The question arises of how to treat the extra cross-coupling inverters when such filters are multiplexed. Such filters are often realized using dual-mode cavities to give convenient means of inclusion of the extra cross couplings.

From a practical viewpoint filters will have at least 10-dB attenuation in the stopband and normally considerably more. This implies that the first cross-coupling is very small compared to the main line couplings, and for filters of degree greater than 2, the second cross-coupling will also be small. Thus, in calculating the input impedance of the filter for the purposes of the multiplexer theory, the first and second cross-couplings may be ignored initially. Then, after calculating the correction terms for multiplexing, it can be shown that the scaling factor for the correction on a cross-coupling J_{kq} is the same at the scaling factor on J_k. For example, the correction factor on J_k for the rth channel is given by (33) as $(1-\gamma_{rkl})^{1/2}$, so that the corresponding cross-coupling admittance inverter changes accordingly as

$$J_{(r)kq} \rightarrow J_{(r)kq}(1-\gamma_{rkl})^{1/2}, \qquad k=1,2,\cdots,N_r-1. \quad (60)$$

Here the subscript r has been added in parentheses to indicate the rth channel as in (33).

B. Design of Practical Waveguide Multiplexers

Early waveguide multiplexers constructed on a common manifold were designed on a semiempirical basis and required adjustable phase shifters between channels to take up unknown junction effects, particularly unpredicted phase shifts across the junctions. This is no longer necessary, since it is not difficult to take the junction effects into account by computer analysis, e.g., [6] which describes the design of an aperture-coupled E-plane multiplexer.

Similar excellent results have been obtained both in theory and practice using aperture-coupled H-plane manifolds. The slit-coupled H-plane T junction is a particularly useful circuit for rectangular waveguide filters since the equivalent circuit is very accurate, and the junction provides the first admittance inverter and shunt susceptance of the filter. The equivalent circuit of Marcuvitz [7, Fig. 6.6-2] is easily transformed as indicated in Fig. 7. Here we make the simplification that the broad dimensions of the main line and side arms are equal, giving

$$\frac{X_b}{Z_0} = \frac{a}{\lambda g}\left[\left(\frac{4a}{\pi d}\right)^2 - 1\right] + \frac{2a}{\lambda_g} \quad (61)$$

$$\frac{X_c}{Z_0} = \frac{2a}{\lambda_g}. \quad (62)$$

The capacitive T of Fig. 7(b) is identical to a series reactance $-j(X_b - X_c)$ in cascade with an ideal impedance inverter of impedance X_c, and carrying out a Kuroda-type transformation gives the final equivalent circuit of Fig. 7(c) where

$$\frac{J}{Y_0} = \frac{\lambda_g}{2a} \quad (63)$$

$$\frac{B}{Y_0} = -\frac{\lambda_g}{4a}\left[\left(\frac{4a}{\pi d}\right)^2 - 1\right]. \quad (64)$$

The negative shift in the reference planes, as indicated in

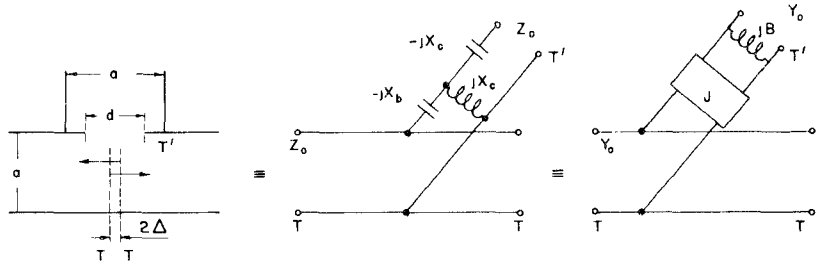

Fig. 7. (a) Slit-coupled H-plane T junction; (b) Marcuvitz equivalent circuit; and (c) Modified equivalent circuit.

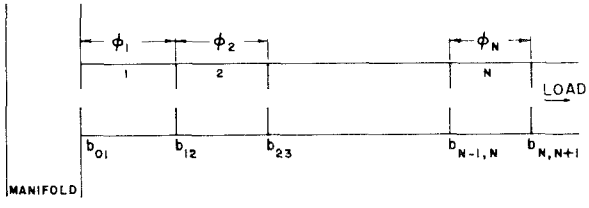

Fig. 8. Typical waveguide channel filter on a manifold.

Fig. 7(a), is given by

$$\Delta = \frac{1}{32\pi}\frac{a}{\lambda_g}\left(\frac{\pi d}{2a}\right)^4. \tag{65}$$

The finite thickness of the iris of width d may be taken into account by inclusion of the short length of waveguide so formed, which may be either below or above cutoff.

The design equations for the susceptances and cavity lengths of a direct-coupled cavity filter connected to the manifold, as illustrated in Fig. 8, may be based on those given in [8] for narrow-band filters. The equations require modification when based on the prototype used in this paper [1, Fig. 2] and are as follows.

Given band-edge guide wavelengths λ_{g1} and λ_{g2}, the fractional bandwidth is defined as

$$w = \frac{2(\lambda_{g1}-\lambda_{g2})}{\lambda_{g1}+\lambda_{g2}}. \tag{66}$$

Defining

$$J_1' = \frac{1}{J_0}\sqrt{\frac{\omega_1' g_1}{(\pi/2)w}} \tag{67}$$

$$J_k' = \frac{1}{J_k}\frac{\omega_1'\sqrt{g_{k-1}g_k}}{(\pi/2)w}, \qquad \text{for } k=2,3,\cdots,N \tag{68}$$

$$J_{N+1}' = \frac{1}{J_N}\sqrt{\frac{\omega_1' g_N}{(\pi/2)w}} \tag{69}$$

then the shunt susceptances are given by

$$b_{01} = J/J_1' - J_1'/J \tag{70}$$

$$b_{k,k+1} = J_k' - 1/J_k', \qquad \text{for } k=1,2,\cdots,N-1 \tag{71}$$

$$b_{N,N+1} = J_{N+1}' - 1/J_{N+1}' \tag{72}$$

$$\phi_k = \pi - 1/2\left(\tan^{-1}\frac{2}{|b_{k-1,k}|} + \tan^{-1}\frac{2}{|b_{k,k+1}|}\right). \tag{73}$$

In (70) above J is the admittance inverter shown in Fig. 8(c), given by (63) with $Y_0 = 1$.

The iris opening d in Fig. 7(a) is given by (64) with B/Y_0 replaced by the value of b_{01} given by (70).

In applying the above formulas to the multiplexer the modified prototype element values given earlier in this section are used, and the cavities are "detuned" from their nominal values given by (73) in accordance with this theory.

In the case of rather broad-band waveguide filters, the improved theory given in [9] should be used to derive equivalent effective prototype values for [67]–[69].

IV. Practical Result: A WR229 Waveguide Triplexer

The theory described in the previous section was applied to the design of a waveguide WR229 manifold triplexer. Each channel consists of a 37-MHz bandwidth six-cavity Chebyshev filter having ripple return loss 26 dB (VSWR 1.1) with center frequencies at 3720, 3800, and 3880 MHz. Although this is not a "severe" contiguous or nearly contiguous case, it is far from trivial from a design viewpoint because the 26-dB return loss is relatively difficult for a multiplexer. The theoretical performance is shown in Fig. 9, which gives the common port return loss and channel insertion losses of the triplexer, taking all practical effects into account. It is seen that all six return loss poles are present in each channel, and the return loss minima are close to the specified level of 26 dB. The physical spacing between channels was approximately one guide wavelength to allow the filters to be all on one side of the manifold, as shown in Fig. 10.

The measured performance was very close to the theoretical prediction, and no problems were experienced in obtaining the five ripples at the 1.1-VSWR level in each channel. In particular, no empirical adjustments to the waveguide manifold were required, e.g., in the relative spacing between the channels. This has been the case also for several manifold multiplexers of this type made in a variety of waveguide sizes.

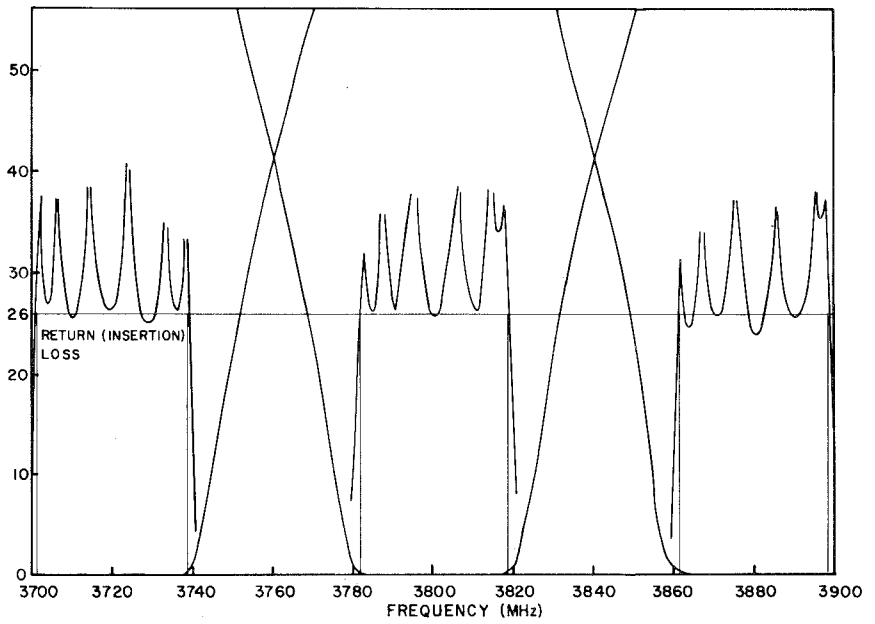

Fig. 9. Analysis of a practical waveguide manifold triplexer.

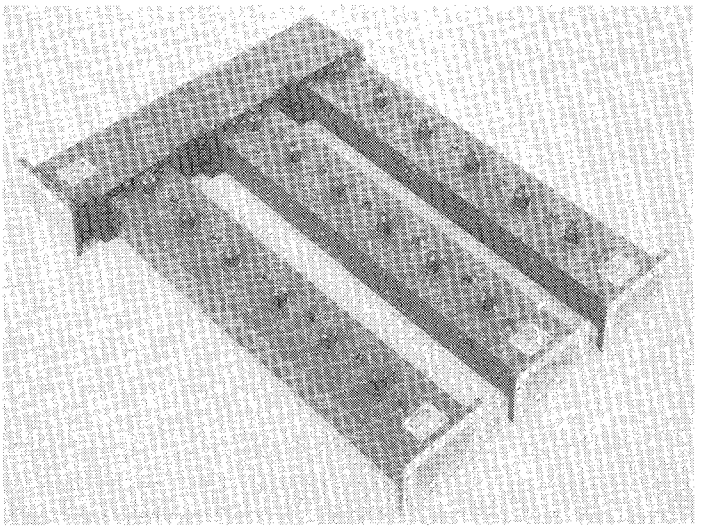

Fig. 10. Photograph of the WR229 triplexer.

V. Conclusions

A new design process has been presented for bandpass channel multiplexers where the channel filters are separated along a manifold. The design process has been found to be valid for a large variety of channel separations from very large guardbands down to contiguous channel operation. In addition to the design process being canonic (i.e., the total degree of the multiplexer is equal to the sum of the individual degrees of the channel filters), a significant improvement in channel performance is achieved over the individual channel filters operating in isolation. For the basic manifold prototype multiplexer with frequency-independent phase shifters, theoretically, there are no limitations upon the number of channels nor the complexity or type of channel filters used.

In practice, the manifold will possess a transmission-line frequency dependence, and modifications to the design process have been presented which are valid for fairly broad-band operation. There are two limitations, namely, the maximum channel bandwidths and the maximum number of channels, the latter normally being more restrictive due to the significant frequency dependence of a long manifold.

Examples have been given indicating that both input and output multiplexers suitable for most communication systems may readily be designed. Practical waveguide manifold multiplexers have been constructed, showing that the theory is reproduced in practice with no empirical adjustments being required to the location of the filters on the manifold.

References

[1] J. D. Rhodes and R. Levy, "A generalized multiplexer theory," this issue, pp. 99–111.
[2] R. J. Wenzel and W. G. Erlinger, "Narrowband contiguous multi-

plexing filters with arbitrary amplitude and delay response," *1976 IEEE MTT-S Int. Microwave Symp. Digest*, IEEE Cat. no. 76CH1087-6MTT, pp. 116–118.
[3] M. H. Chen, F. Assal, and C. Mahle, "A contiguous band multiplexer," *Comsat Tech. Rev.*, vol. 6, no. 2, pp. 285–305, Fall 1976.
[4] J. D. Rhodes, "Direct design of symmetrical interacting bandpass channel diplexers," *Inst. Elec. Eng. Microwaves, Opt., Acoust.*, vol. 1, no. 1, pp. 34–40, Sept. 1976.
[5] R. Levy, "Filters with single transmission zeros at real or imaginary frequencies," *IEEE Trans. Microwave Theory Tech.*, vol. MTT-24, pp. 172–181, Apr. 1976.
[6] A. E. Atia, "Computer-aided design of waveguide mutiplexers," *IEEE Trans. Microwave Theory Tech.*, vol. MTT-22, pp. 332–336, Mar. 1974.
[7] N. Marcuvitz Ed., *Waveguide Handbook*. M.I.T. Radiation Lab. Series, vol. 10. New York: McGraw-Hill, 1951.
[8] S. B. Cohn, "Direct-coupled-resonator filters," *Proc. IRE*, vol 45, pp. 187–196, Feb. 1957.
[9] R. Levy, "Theory of direct-coupled-cavity filters," *IEEE Trans. Microwave Theory Tech.*, vol. MTT-15, pp. 340–348, June 1967.

Tables for Nonminimum-Phase Even-Degree Low-Pass Prototype Networks for the Design of Microwave Linear-Phase Filters

J. H. CLOETE, MEMBER, IEEE

Abstract—**The element values of a selection of even-degree nonminimum-phase low-pass prototype networks with equiripple passband amplitude and constant group delay in the least squares sense over a large percentage of the passband are tabulated. All the prototypes have passband insertion loss ripple $R = 0.01$ dB and cutoff frequency $\omega_c = 1.0$ rad/s at the 0.01-dB point. Five tables contain the element values of networks up to degree $N = 20$. The tables are classified according to the number of transmission zeros at infinite frequency NZ_∞ and the passband frequency to which the group delay is constant in the least squares sense ω_d. The following combinations of NZ_∞ and ω_d are tabulated: $NZ_\infty = 2$ and $\omega_d = 0.9$; $NZ_\infty = 4$ and $\omega_d = 0.8$; $NZ_\infty = 6$ and $\omega_d = 0.7$; $NZ_\infty = 8$ and $\omega_d = 0.6$; and $NZ_\infty = 10$ and $\omega_d = 0.5$. The maximum phase and delay errors for each network are tabulated. Plots of the passband group delay and stopband insertion loss versus frequency, for each network, accompany the tables to facilitate selection of a prototype. The prototypes are suitable for the design of narrow-band generalized interdigital, generalized direct-coupled cavity waveguide, and generalized combline linear-phase filters. A simple algorithm for the analysis of the prototypes is given.**

I. Introduction

THE SYMMETRICAL nonminimum-phase low-pass prototype network introduced by Rhodes [1] is shown for the even-degree case. It is topologically suited to the design of microwave bandpass filters capable of good amplitude selectivity while approximating closely to linear phase over a large percentage of the passband. The microwave filters are realized by providing coupling between nonadjacent resonators. Examples include the generalized interdigital filter [2], the generalized direct-coupled cavity waveguide filter [3]–[5] and the generalized combline filter [6].

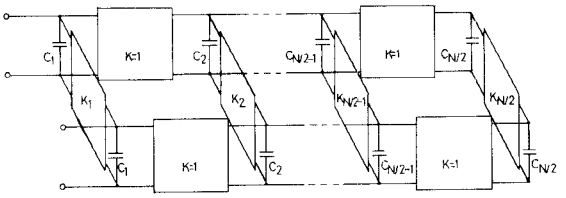

Fig. 1. The symmetrical even-degree nonminimum phase low-pass prototype network consisting of lumped capacitors and ideal admittance inverters. The notation for the network elements is consistent with the notation used in Tables I–V.

The first step in the design of a narrow-band microwave linear-phase filter is to find the element values of a low-pass prototype which satisfies the amplitude and phase or group delay specifications. When this step is completed the elements in the equivalent circuit of the microwave filter may be calculated [2], [3]. A number of approximation theories and techniques have been described for the construction of nonminimum-phase low-pass transfer functions from which the element values of the prototype networks can be synthesized [1], [4], [7]–[10]. These methods generally require considerable computation to achieve a satisfactory prototype. The method of Levy [4], applicable when only one pair of finite zeros provides

Manuscript received February 13, 1978; revised June 27, 1978.
The author was with the Department of Electrical Engineering, University of Stellenbosch, Stellenbosch 7600, South Africa, on leave from the National Institute for Aeronautics and Systems Technology, Council for Scientific and Industrial Research, P.O. Box 395, Pretoria 0001, South Africa.

0018-9480/79/0200-0123$00.75 ©1979 IEEE